DURABILITY AND DEBOND EVALUATION OF HIGH-RISE CONCRETE BUILDINGS USING INFRARED THERMOGRAPHY

W. L. Lai [1,2], and C. S. Poon [1] [1]
[1] Department of Civil and Environmental Engineering, The Hong Kong Polytechnic University, Hong Kong
[2] Department of Land Surveying and Geo-infomatics, The Hong Kong Polytechnic University, Hong Kong.

ABSTRACT

The paper presents the development of a passive infrared thermography (IRT) method as a screening tool to indicate and measure the size of debonds in external wall envelop of building structures. The underlying principle of this method is the comparison of the surface temperature at areas with heat trapped by air (debond) during and after exposure to sunlight with the cooler areas (without debond). Mathematical inversion of the heat distribution over an external wall surface enables the measurement and calculation of debond size and boundary. It has been proven that the proposed methodology and algorithm are accurate, and can be used generally because they are not affected by factors like depth of debond, sizes of debond, surface temperatures, temperature scales set in the infrared camera and time when the thermograms are taken. This quantitative method allows the evaluation of the long term durability and facilitates planning of rehabilitation of tall buildings.

KEYWORDS

Infrared thermography, debond of wall finishes, high-rise building

INTRODUCTION

Residential buildings in Asian cities are probably the tallest and most densely populated in the world. The envelop of tall buildings rendered by tile-adhesive requires debond evaluations for short-term assessment of tile-falling hazards and long term rehabilitation. To date, the evaluations are often based on three traditional assessment methods: visual inspection, hammer-tapping and pull-off tests. Early warning of tile-adhesive failure cannot be provided by these methods. The drawbacks may be overcome by passive infrared thermography (IRT) which makes use of the Sun as a thermal stimulus to differentiate the colder bonded and hotter debonded areas non-destructively, remotely and effectively. The underlying principle is that air in the debonded area renders a hotter surface temperature than the areas without debonds after a period of exposure to natural sunlight. So when a non-uniform temperature distribution is observed, it may indicate the presence of debonds, after excluding other factors such as effects of other heat sources, variations of emissivity of the concerned materials, etc [1-4]. However despite the passive IRT is available to identify debond *qualitatively* and progressively gain acceptance for almost 10 years in Hong Kong, a quantitative method for estimation of the boundaries and sizes of the debond is still lacking. A quantitative method is needed to estimate extent of deterioration and cost of rehabilitation, and provide basis for indentifying of defects before detailed pull-off tests or hammer tapping are deployed. The lack of a quantitative method is because such method requires sophisticated programming skills and in-depth understanding of the transient heat transfer occurring in the materials which are beyond the experience of most practitioners and engineers.

The major advantage of the quantitative over qualitative IRT assessment is that the former does not require an artificially adjusted temperature range to visualize the hot and cold region in a thermogram. Such an adjustment in qualitative IRT is purely based on the experience of the operator and does not follow any established guidelines. In practice, a narrower range means more debond while a broader range means less debond. As a result, it may lead to misleading interpretations because the users can manipulate the extent of severity of debond, via adjustment of the temperature range. Currently, such subjective adjustment is not standardised nor regulated in most international or local codes of practice. In this paper, we propose a systematic image processing method to carry out the quantitative IRT assessment of debonds. The method is based a processing technique using linear gray-scale images with spatial pixel/temperature differentiation methods developed by the authors in the assessment of CFRP-concrete composites previously [5-7]. A clear advantage of this method

is that the temperature/pixel's differentiation process is independent of the absolute temperature/pixel values, and therefore does not require the subjective manipulation of temperature scale mentioned above. The paper also presents the results of study the effects of four factors , namely depth of debond, sizes of debond, surface temperatures, temperature scales set in the infrared camera and time when the thermograms are taken, on the accuracy of the quantitative IRT assessment.

MATERIALS

A concrete wall with sizes of 3m long x 2m wide x 200mm thick was fabricated and placed (facing south east) on the roof of a building, as shown in Figure 1. The wall surface was rendered with a 25mm thick proprietary base plaster (Optimix, BP126) [8]. Within the wall, six circular plastic foam plates (artificial defects) with two different sizes (7.5cm and 15cm) at three cover depths (5mm, 7mm and 11mm) were embedded. These artificial defects could not be seen by naked eyes (Fig. 1), but were clearly visible with the infrared camera in non-linear colour (Figure 2, left) and linear gray scale (Figure 2, right). The wall faced south east and hence, it received heat energy from the Sun in the morning. The passive IRT measurement was carried out from 10:30am to 01:15pm after about 4 hours of direct sunlight irradiation.

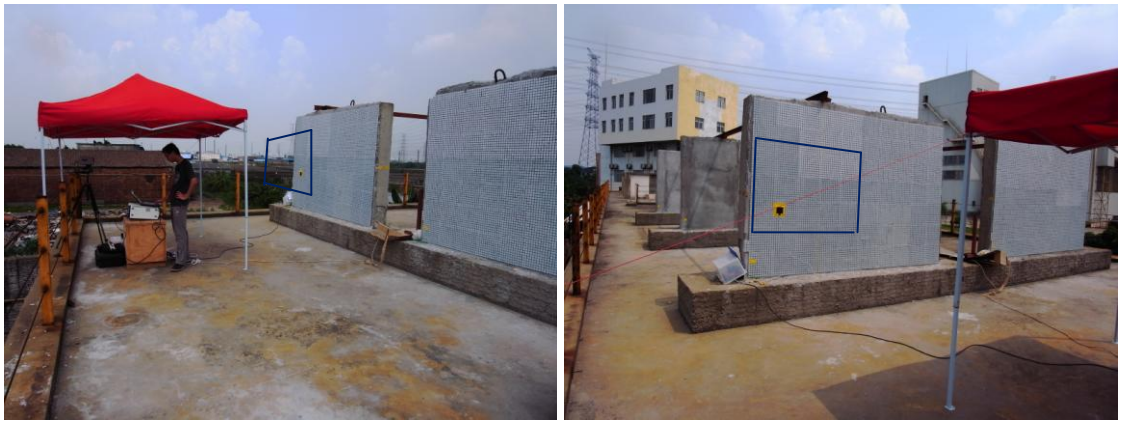

* the blue area is the studied area covered by the infrared camera.

Figure 1 Setup of the wall panel

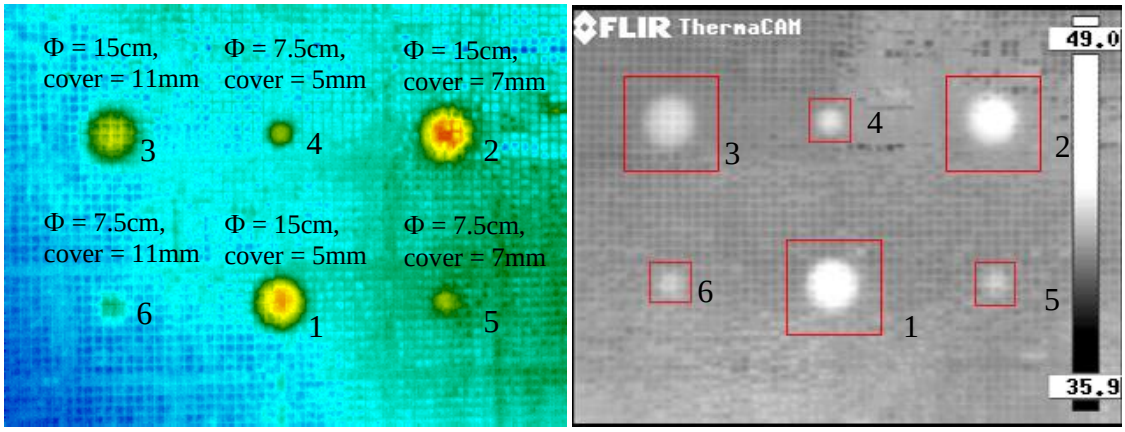

Figure 2 Colour (left) and gray (right) scale thermograms

MEASUREMENT METHODOLOGY

The quantitative assessment of debonds comprised two steps: (1) qualitative detection by recognizing non-uniform distribution of white, gray and black colors over the thermogram and (2) size and boundary quantification by computer processing. The first step was based on a time-lapsed collection of thermograms over the concrete wall surfaces using a FLIR quantum well SC3000 infrared thermo-imager. The thermograms were captured once every 15 minutes, at which time there were changes of (i) relative angles between the sun and the wall, and (ii) surface temperatures. The Infrared camera and instrumentation were controlled by National Instrument's hardware and an in-house developed LabVIEW program.

The second step of the assessment started by the selection of regions of interest (ROI) as shown by the red rectangles in Figure 2, and digitizing the gray scale infrared images (Figure 3, left). The image arrays were firstly filtered by a median filter which took the average of 10 neighbouring pixel values, so as to eliminate the noise induced by the tile joints contained in the images (Figure 3, right). The filtered images were then processed with a spatial pixel differentiation method. This method was developed based on our previous work on CFRP-concrete composites [5-7, 9], and is described in details as follows.

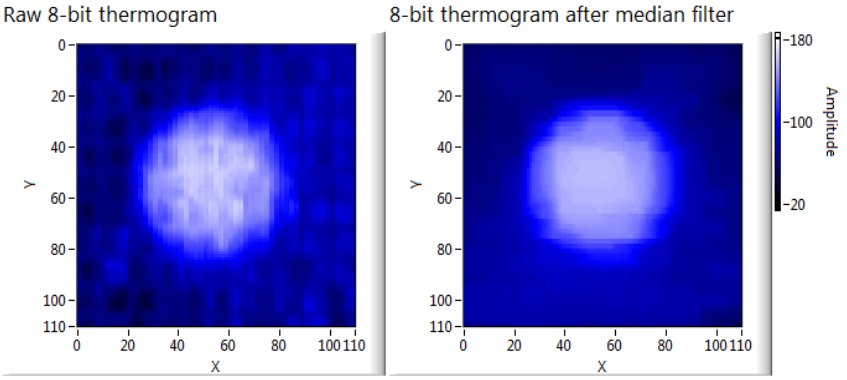

Figure 3 Raw image (left) and filtered image (right) in a ROI

The filtered images were further processed to define the positions of steepest temperature gradient computed over the debonds [1,10]. This computation may be processed with a number of algorithms, such as Roberts gradient [11], high degree approximation [1], second order fit [1], inflection point [5-7,12]. With this method, the absolute temperature/pixel values or temperature/pixel range selected in the thermograms were not used in image processing. Therefore, the limitation of IRT applications due to artificially adjusted temperature scale discussed in Section 1 can be overcome.

In this paper, we elected to carry out the pixel differentiation algorithm based on a second order fit method [1]. Within the selected ROI (i.e. red rectangles in Fig. 2, right), the 8-bit pixel values P(y) and P(x) (Fig. 2, right) in each column and row along the vertical and horizontal directions of the debond was extracted for processing respectively. Each point in P(y) and P(x) was differentiated to position the maximum gradient, or debond boundary at y' and x' and calculation of debond width L_y and L_x as shown in Fig. 4. The computation is shown in Eq [1] and [2].

$$\frac{\partial P(y)}{\partial y} = \text{y' (max) and y' (min) at y-cut;} \quad \frac{\partial P(x)}{\partial x} = \text{x' (max) and x' (min) at x-cut;} \quad \text{.....[1]}$$

$$L_x = \left| x'(\max) - x'(\min) \right| \text{ and } L_y = \left| y'(\max) - y'(\min) \right| \text{.....[2]}$$

where y and x = pixel cell; P(y) = pixel intensity/temperature as a function at any pixel cell 'y'; P(x) = pixel intensity as a function at any pixel cell 'x'; L_x and L_y are the length of debond.

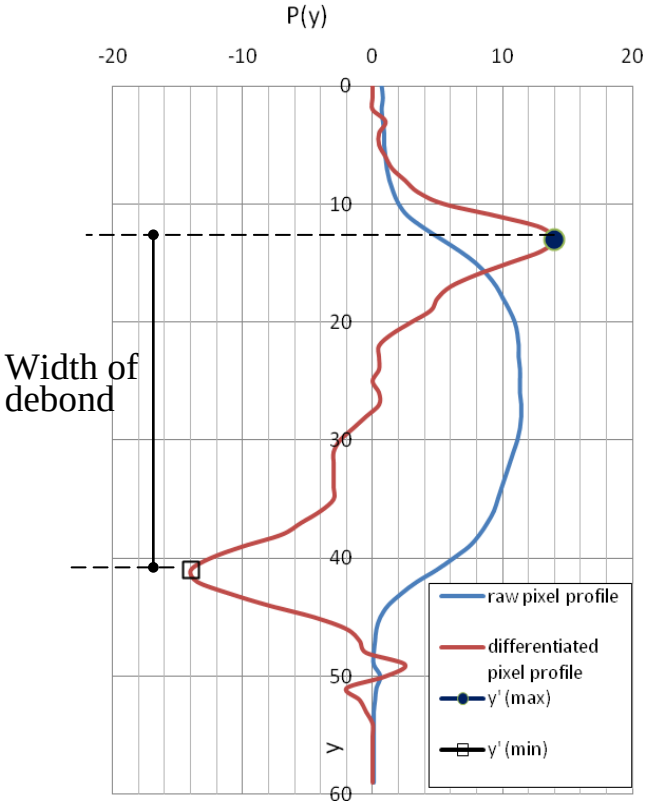

Figure 4 Pixel profile after median filter and differentiation

With the positions y' (max), y' (min), x'(max) and x'(min) at every column of P(y) and P(x) defined respectively, the original images were transformed to binary scale images revealing only the intact and debond areas as shown in Figure 5. In this figure, '1' (the white color) means debond and '0' (or the black color) means intact. Binary images from the x-cut and y-cut in equation [1] are individually generated (Figure 5, left and middle), and combined through a 'AND' and 'OR' gate (Figure 5, right). The 'AND' gate refers to the positions at any coordinate that are defined as debond when BOTH the binary value obtained from x-cut or y-cut are equal to the value '1'. The 'OR' gate means that the positions at any coordinate are defined as a debond when EITHER the binary value obtained from x-cut OR y-cut is equal to the value '1'. All remaining value not fitting these criterion is defined 'intact' and remain '0' in the combined binary thermogram (Figure 5, right). Finally, the number of debond pixels was counted and used for computation of the actual debond area after proportioning the number of pixels in the image to the actual width of the panels.

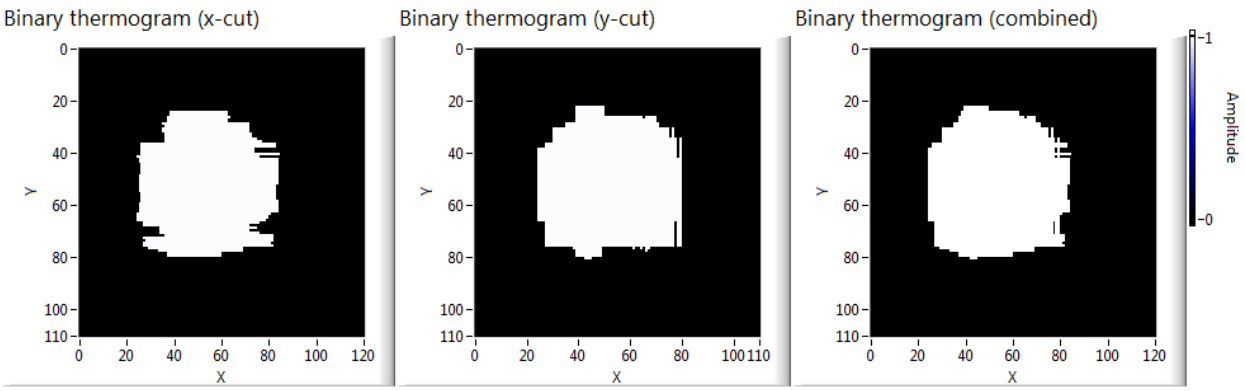

Figure 5 X-cut, Y-cut and combined binary thermograms revealing debond and no debond within the ROI

RESULTS AND DISCUSSION

In the above study, the heat transfer mechanism and non-uniform temperature distributions are governed by the embedded plastic foam plates (which simulate debond). The foam plates acted as insulation layers to obstruct the passage of the incident thermal wave. As a result, the surface of the concerned areas exhibit higher surface temperatures than the other intact areas, as shown in Figure 2. The two most important factors that control the intensities of heat absorption are the cover depth of the embedded plates (defects) and the sizes of the plastic foam plates. For cover depth, the closer the plate to the surface is (e.g. 5 mm compared to 7 mm in Figure 2), the more obvious and stronger the intensity would be. For sizes of the foam plate, a foam plate with a larger size (150mm diameter) also shows a stronger intensity than a foam plate with a smaller size (75mm diameter). The above analysis provides a qualitative detection of the debonds because it is based on comparing the observed surface temperatures based on an arbitrary adjustment of temperature scale discussed in Section 1.

When the size and boundary of the debond are required to be quantified, the methodology and algorithm of pixel/temperature differentiation discussed in Section 3 are used to generate binary thermograms for size measurement and the results are shown Table 1. Debond No. 1 to 4 are easily determined because of the better signal to noise ratio, as a result of their larger size (15cm diameter in debond 1-3) or shallower cover depth (5mm in debond 4). Debond No. 5 and 6 are however, not quantifiable by the method because of the low signal to noise ratio which is probably related to the small size of the debond (7.5cm diameter) and the relatively deep cover depths (7 and 11 mm)

The measured values of the debond sizes are summarized in Table 1. These values are very comparable to the actual sizes (176.7cm^2 and 44.2cm^2). The results show that the percentage errors are at most 7.9% in all measurable cases. This suggests that variations in embedded depth (5/7/11mm), sizes of debond (7.5/15cm), temperature range during IRT (33.9-44/37.1-45.9/35.9-49^{0}C) or the time when the thermograms were taken (10:30am to 1:15pm) do not affect the accuracy on the size determination of the debonds. It also suggests that the quantitative inversion method can be used generally and is not limited by any of the above mentioned factors, nor by the absolute values of the surface temperatures.

Debond No.		1	2	3	4	5	6
Diameter of debond (cm)		15	15	15	7.5	7.5	7.5
Size of debond (cm^2)		176.7	176.7	176.7	44.2	44.2	44.2
Cover depth (mm)		5	7	11	5	7	11
Time	Temperature range (^{0}C)	Measured sizes of debond (cm^2)					
1030	33.9 - 44	169.6	199.2	166.3	49.8	-	-
1045	33.9 - 44	165.5	172.9	166.4	48.7	-	-
1100	33.9 - 44	163.6	192.8	174.4	49.5	-	-
1115	37.1 – 45.9	172.4	162.0	175.6	43.4	-	-
1130	37.1 – 45.9	165.9	192.7	169.4	44.7	-	-
1145	37.1 – 45.9	166.4	157.2	169.6	42.2	-	-
1200	35.9 – 49	171.5	164.8	178.1	38.3	-	-
1215	35.9 – 49	169.6	169.9	174.3	42.3	-	-
1230	35.9 – 49	166.5	163.2	174.1	44.1	-	-
1245	35.9 – 49	167.7	163.9	168.0	40.5	-	-
1300	35.9 – 49	164.6	172.1	171.5	43.0	-	-
1315	35.9 – 49	169.6	165.6	183.9	42.2	-	-
RMSD		**2.8**	**14.0**	**5.2**	**3.6**	-	-
% error		**1.6**	**7.9**	**2.9**	**2.0**	-	-

Remark: The debond No. corresponds to those in Figure 2.

CONCLUSIONS

A methodology and algorithm of both qualitative and quantitative assessments of debonds in tiled wall finishes by passive infrared thermography is presented. The method enables the evaluation of extent of debonds in these wall finishes. The method avoids the use of arbitrary adjustment of temperature scale in the traditional

qualitative assessment. It has been shown to be independent of variations of the depth and sizes of debond, the surface temperatures, the temperature scales set in the infrared camera and the time when the thermograms are taken. The results show that the error of debond size estimation is within 7.9% and is considered to be very accurate in non-destructive evaluations. Other factors that may also affect the results (e.g. angle of illumination, wind speed, variation of emissivity of the materials, types of thermo-imagers, etc.), are currently under investigation to further improve the accuracy of the developed methodology and algorithm.

ACKNOWLEDGMENTS

The authors wish to thank the funding support of the Innovative Technology Fund, HKSAR Government, and Optimix Cement Connections Ltd. for providing the plastering materials.

REFERENCES

[1] Maldague, X. P. V. Theory and Practice of Infrared Technology for Nondestructive Testing, Wiley-Interscience, John Wiley & Sons, Inc. 2001.

[2] ACI 2282r-98, Nondestructive Test Methods for Evaluation of Concrete in Structures

[3] BS EN 13187:1998 Thermal performance of buildings - Qualitative detection of thermal irregularities in building envelopes - Infrared method

[4] Hong Kong Concrete Institute, Test Method for Evaluation of Building Exterior Wall Finishes using Infrared Thermal-Imaging Technique, 2009.

[5] W.L. Lai, S. C. Kou, C.S. Poon, W.F. Tsang, S.P. Ng and Y.Y. Hung. Characterization of flaws embedded in externally bonded CFRP on concrete beams by infrared thermography and shearography, *Journal of Nondestructive Evaluation*, Volume 28, pp. 27–35, 2009.

[6] W.L. Lai, S. C. Kou, C.S. Poon, W.F. Tsang, C. C. Lai. Effects of elevated temperatures on interfacial delaminations, failure modes and shear strength in externally-bonded CFRP beams using infrared thermography, gray-scale images and direct shear test, *Construction and Building Materials*, Volume 23, pp. 3152–3160, 2009.

[7] W. L. Lai, S. C. Kou, C. S. Poon, W. F. Tsang, C. C. Lai. Characterization of the Deterioration of Externally Bonded CFRP-Concrete Composites using Quantitative Infrared Thermography, *Cement and Concrete Composites*, 32(9): 740-746, 2010.

[8] Optimix, BP126 base plaster product catalogue.

[9] W.L. Lai, S. C. Kou, Poon C.S., Tsang W.F., Ng S.P. and Hung Y.Y. Characterization of flaws embedded in externally bonded CFRP on concrete beams by infrared thermography and shearography, *Journal of Nondestructive Evaluation*, 28: 27–35, 2009.

[10] Krapez, J.C. and Cielo, P. Thermographic nondestructive evaluation: data inversion procedures part I: 1D analysis, *Res. Nondestructive Evaluation*, 1991, 3(2), 81-100.

[11] Gonzalez, R.C. and Wintz, P. Digital Image Processing, 2nd Ed. Addision-Wesley, Reading, MA, 1987.

[12] Starnes, M.A., Carino, N.J., Kausel, E.A. Preliminary Thermography Studies for Quality Control of Concrete Structures Strengthened with Fiber-Reinforced Polymer Composites. Journal of Materials in Civil Engineering, Volume 15, No. 3, pp. 266-273, 2003.